ELSEVIER

Polymer 41 (2000) 7067–7082

polymer

Hybrid blends of similar ethylene 1-octene copolymers

Dipak Rana[1], Hak Lim Kim, Hanjin Kwag, Soonja Choe*

Department of Chemical Engineering, Inha University, Inchon 402-751, South Korea

Received 2 February 1999; received in revised form 25 June 1999; accepted 4 January 2000

Abstract

Two binary blends of FA + FM and SF + FM comprising ethylene 1-octene copolymers (EOC), one component prepared by Ziegler–Natta and another by metallocene catalysts were investigated in terms of the thermal, viscoelastic, rheological, mechanical, and morphological properties. The big difference between the Ziegler–Natta and metallocene catalyzed EOCs is the distribution and the length of the side chain branching. Each component in FA + FM has similar melt index (MI), density, and comonomer content, while that of the second pair (SF + FM) has similar MI and density, but differs in comonomer content. Both the melt and solution blended materials exhibit two distinct melting and crystallization peaks, implying that the constituents exclude one another during crystallization. A single β relaxation shifted to lower temperature with the content of metallocene EOC, indicates miscibility in the amorphous region, while the γ transition is observed in the same position within experimental error. Rheological observations suggest the FA + FM to be miscible, but not SF + FM, implying that the difference in the distribution and the length of the side chain branching influences the melt properties of the EOC blends regardless of the similarity in the density and MI. In addition, no dependency of comonomer contents and the difference in the side chain branching on the mechanical properties is observed. Morphological studies observed from the slow cooled specimens show large spherulitic diameter and ring space for the Ziegler–Natta EOC. In particular, grass like spherulitic sheaf structure is dominated in the blend by the addition of metallocene EOCs. Hence the properties of the hybrid blends consisting of similar MI and density are influenced by not only the distribution of the comonomer, but also the length of the side chain branching.

Keywords: Ethylene-1-octene copolymer (EOC); EOCs blend; Ziegler–Natta and metallocene catalysts

1. Introduction

Polyolefins are the volume leaders of polymers in the industrial field. A vast amount of blends containing the linear low-density polyethylene (LLDPE) have been commercially used in the agricultural application and packaging industry. In general, LLDPE is a copolymer of 1-butene, 1-hexene or 1-octene comonomer with ethylene. It is known that the distribution of comonomer in polyolefin cannot be controlled with the Ziegler–Natta catalyst, whereas uniformly distributed comonomer can be achieved using the metallocene catalyst. The Ziegler–Natta catalyst, which is multi-site in nature, results in the heterogeneous distribution of comonomer units, whereas the metallocene catalyst that contains catalytic sites, which are identical, brings about a uniform distribution of the comonomer. It is well established that the compatibility of polyolefin blends is dependent on their chain structure. Although much research has been devoted to polyolefin blends [1–12] containing LLDPE made by the Ziegler–Natta catalyst, more work is needed for the recently developed LLDPE made by the metallocene catalysts.

There are many reports regarding polyolefin blends [13–24]: for example, ultra-low density polyethylene (ULDPE) exhibits broad β relaxation in the dynamic mechanical analysis at sub-ambient temperature and shows superior low temperature impact property [13–15]. Blends of ethylene-1-octene elastomers containing low percentage of 1-octene comonomer form separate crystals in the crystalline region whereas solid state phase behavior in the amorphous region depends on the comonomer content. If the branch concentration of two copolymers is highly different, non-crystalline regions may not be miscible. Miscibility of non-crystalline regions in polyolefin blends produced synergistic effect on the tensile strength [16,17]. High and low molecular weights of high-density polyethylenes (HDPE) made by the metallocene catalyst are found to be miscible themselves from rheological measurements although their molecular weights are different [18,19]. HDPE found to be more miscible with LLDPE made by the Ziegler–Natta catalyst than with LLDPE made by the metallocene catalyst

* Corresponding author. Tel.: + 82-32-860-7467; fax: + 82-32-872-0959.

[1] Present address: McMaster University, Department of Chemistry, Hamilton, Ontario, Canada L8S 4M1.

0032-3861/00/$ - see front matter
PII: S0032-3861(00)00066-5

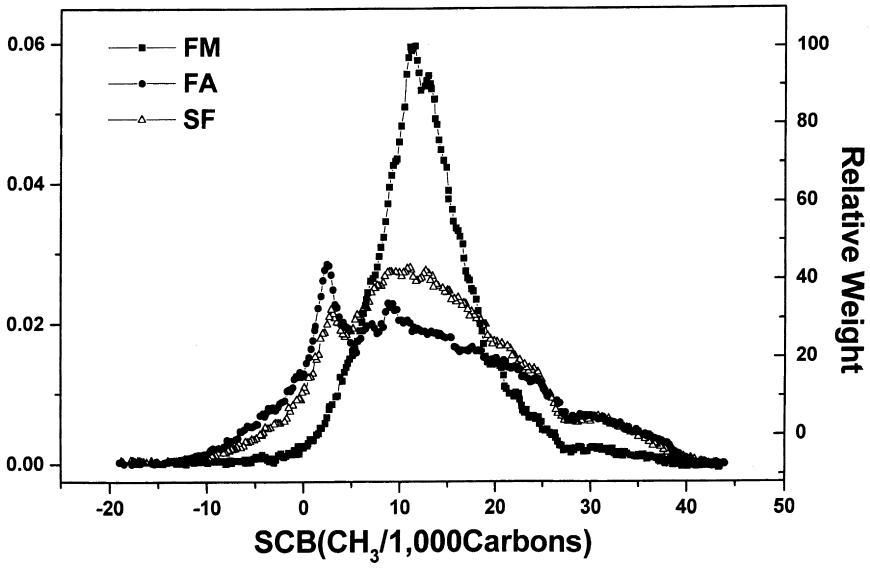

Fig. 1. Side chain distribution of the polymers used in this study.

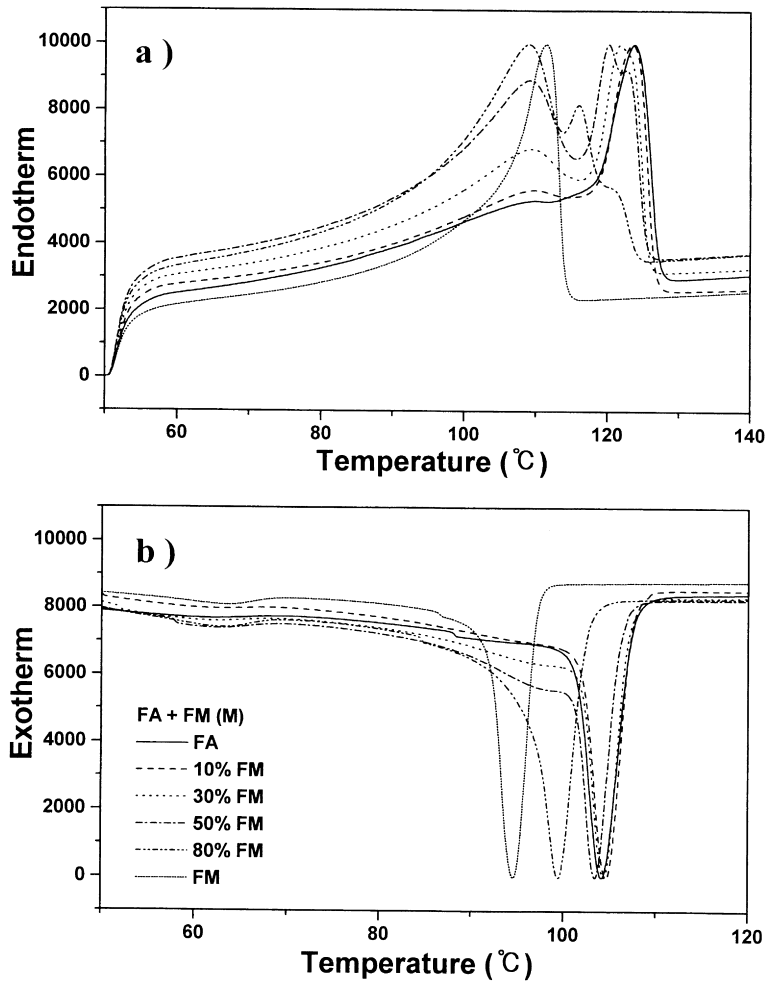

Fig. 2. Melt blended FA + FM systems: (a) melting; and (b) crystallization behaviors in the second scan of DSC thermogram. The number indicates the percentage of second component (metallocene catalyzed EOC) in the blends.

Table 1
The characterization data of the polymers used in this study

Polymer	FM	FA	SF
Supplier	Dow	SK Corp.	Hyundai Petroleum
Grade name	FM1570	FA811U	SF318
MI (g/10 min)	1.0	1.0	1.2
Density (g/cm^3)	0.915	0.919	0.918
Comonomer (1-octene) content (wt%)	7.5	6.5	11.2
Number of side chain branching (CH_3 per 1000 carbons)	12–13	12–13	12–13
Relative molecular weight of the side chain branching	100	40	38
$M_n \times 10^4$	8.18	7.82	7.17
$M_w \times 10^5$	2.08	3.24	2.19
PDI	2.54	4.14	3.06
T_m (°C)	111.3	123.7	108,121,123
T_c (°C)	94.7	104.2	100
ΔH_m (J/g)	118.9	125.1	127.3
ΔH_c (J/g)	107.0	113.0	116.4

[20]. In systematic studies of ethylene copolymers [16,21,22], the fraction of conventional heterogeneous LLDPEs influenced by the short-chain branching content and the comonomer content strongly affected the crystallization and melting behavior, and the degree of crystallinity of the fractions.

After systematic studies on miscibility and processability of LLDPE made by the Ziegler–Natta catalyst with other conventional polyolefins in this laboratory [23–28], our present work is concentrated in examining the effect of the catalyst used for synthesizing the polymers and the influence of the comonomer contents and the side chain distribution on the ethylene-1-octene copolymer (EOC) blends in respect of the thermal, viscoelastic, rheological, mechanical and morphological characteristics. In particular, miscibility based on viscoelastic and rheological observations and phase morphology were discussed. Two model blend systems are selected: one is composed of FA + FM, which are made by the Ziegler–Natta and metallocene catalysts, respectively. Each of them is an EOC having similar

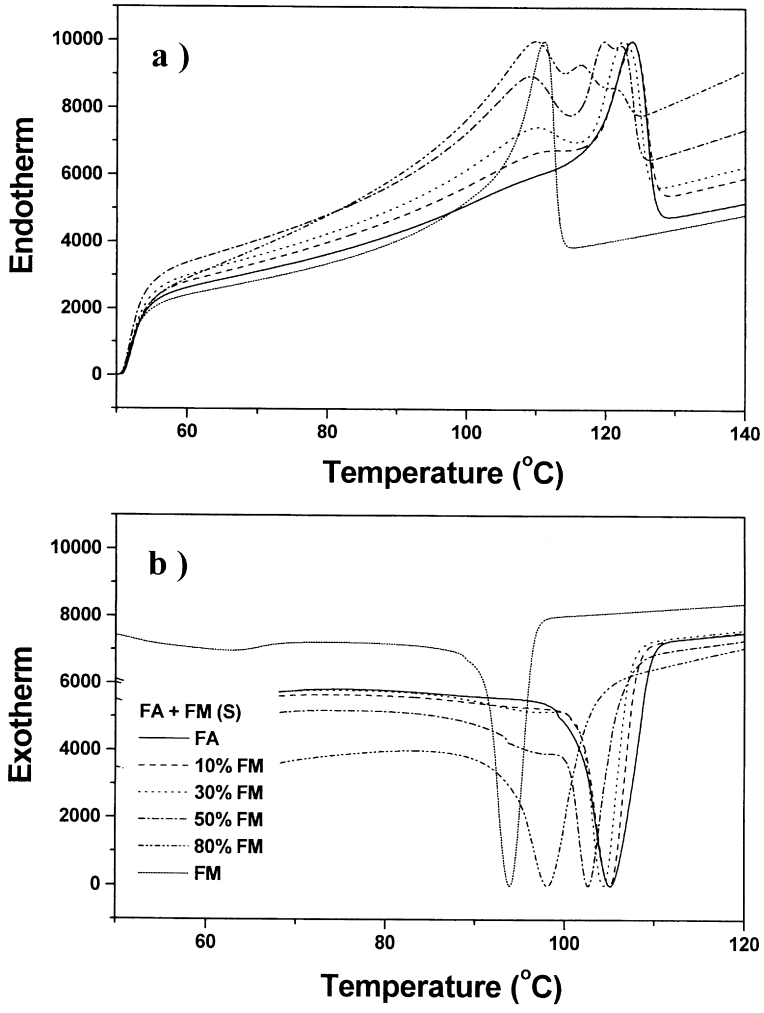

Fig. 3. Solution blended FA + FM systems: (a) melting; and (b) crystallization behaviors in the second scan of DSC thermogram. The number indicates the percentage of second component (metallocene catalyzed EOC) in the blends.

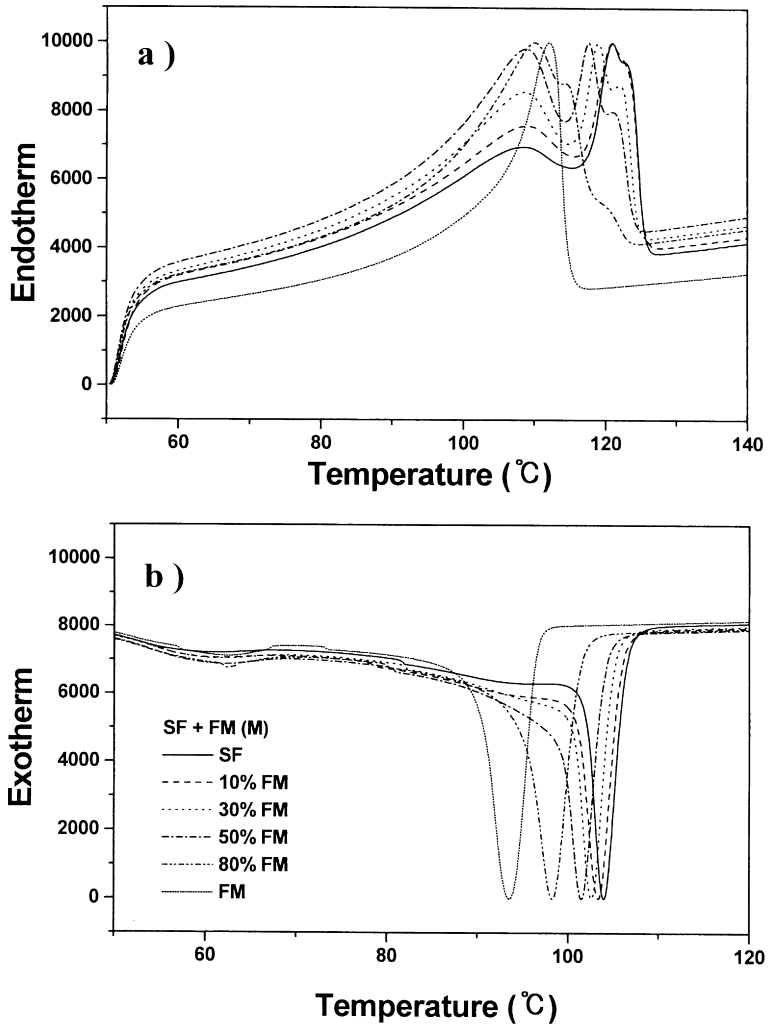

Fig. 4. Melt blended SF + FM systems: (a) melting; and (b) crystallization behaviors in the second scan of DSC thermogram. The number indicates the percentage of second component (metallocene catalyzed EOC) in the blends.

melt index (MI), density, and comonomer content. The other blend pair is composed of SF + FM, which has similar MI and density, but different comonomer contents.

2. Experimental

2.1. Materials and blend preparation

The polymers used in this study are of commercial grades. Ziegler–Natta catalyzed ethylene 1-octene copolymers (EOCs), FA and SF, are the products of SK Corporation and Hyundai Petroleum Chemicals, respectively, Korea. FM, a metallocene catalyzed EOC, is the product of Dow Chemicals, USA. The density, the MI, and the composition of comonomer (by wt%) were provided by the manufacturers. The information of these polymers and abbreviation of each specimen for convenience are listed in Table 1.

The blends of FA with FM (FA + FM) and SF with FM (SF + FM) were melt blended in proportion to weight ratios 100/0, 80/20, 50/50, 30/70, 10/90 and 0/100. A twin screw extruder (Brabender PL 2000) was used at a counter rotating mode with a high mixing condition. The temperature profiles were 190, 200, 210°C for the feed zone, the compression zone, and the metering and die end, respectively. The screw speed was held at 50 rpm and the extruded materials were pelletized after passing through cold water at 25°C. The same processing conditions were given to the pure polymers to make specimens.

Required amount of pure polymers and the blends with the Ziegler–Natta and metallocene catalyzed polyethylene was dissolved in boiling xylene at 140°C and the solution was refluxed for 10 min. Then the solution was precipitated into methanol at room temperature, dried in air oven at 40°C and further dried in vacuum oven at 40°C for 72 h. Dried materials were directly used for thermal studies, whereas the required dimension of the specimens were prepared for viscoelastic and rheological characterization by using a Carver laboratory hot press. The resin was melt pressed in

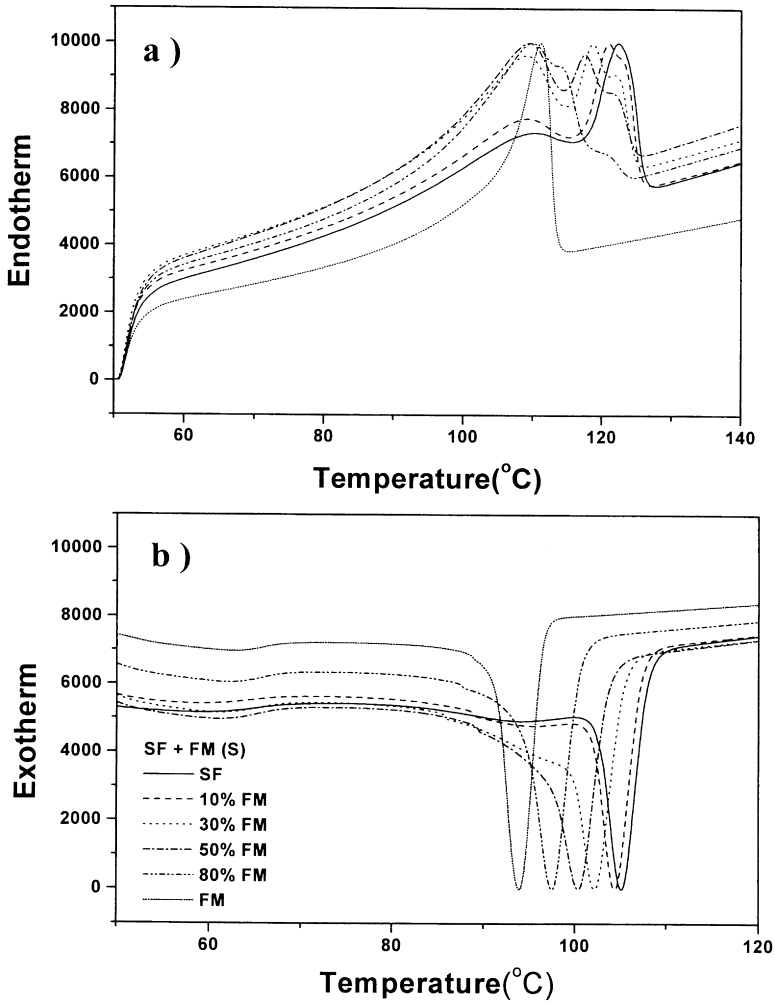

Fig. 5. Solution blended SF + FM systems: (a) melting; and (b) crystallization behaviors in the second scan of DSC thermogram. The number indicates the percentage of second component (metallocene catalyzed EOC) in the blends.

a Carver laboratory hot press at 190°C for 5 min at 2×10^4 Pa pressure and allowed to cool by two ways of cooling processes under atmospheric pressure: one is the fast cooling by soaking in ice-water; and the other is the slow cooling by letting the specimen to cool down on the hot press by turning off the electricity. The specimens were cut parallel to the radial direction.

2.2. Measurements and instrumental analysis

The molecular weights of the polymers were measured by using Waters GPC 150C at 140°C in a solvent of 1,2,4-trichlorobenzene and the monodisperse molecular weight of polystyrene is used as standards. The number average molecular weight (M_n), weight average molecular weight (M_w), and polydispersity index (PDI, M_w/M_n) were calculated from the GPC curves. The molecular weight data of the polymers are listed in Table 1.

The average number of side chain branching and the distribution of it were measured by the temperature rising elution fractionation system using the CAP-TREF of POLYMICS, USA, and the result is drawn in Fig. 1. This figure gives the following information: the first feature is that the average number of side chain branching (SCB: the number of CH_3 per 1000 carbons) in the former two samples, FA and SF, and that of the latter component, FM, seem to be 12–13 side chains per 1000 carbons), but the distribution of the former two is broader than the latter. The second is that the relative molecular weight of the side chain branching of the metallocene EOC is about twice as much large than the Ziegler–Natta catalyzed ECOs, suggesting that the side chain of the metallocene EOC consist of two octenes.

Melting and crystallization behaviors of the blends were studied using a Perkin–Elmer DSC-7 instrument. Indium and zinc were used for the calibration of the melting temperature and the enthalpy of fusion. The samples were scanned up to 180°C at a heating rate of 10°C/min, annealed for 5 min and cooled to 50°C at a cooling rate of 10°C/min, then re-scanned at the same rate and temperature interval. The melting temperature (T_m), the crystallization temperature (T_c), the heat of fusion (ΔH_m) and the heat of crystallization

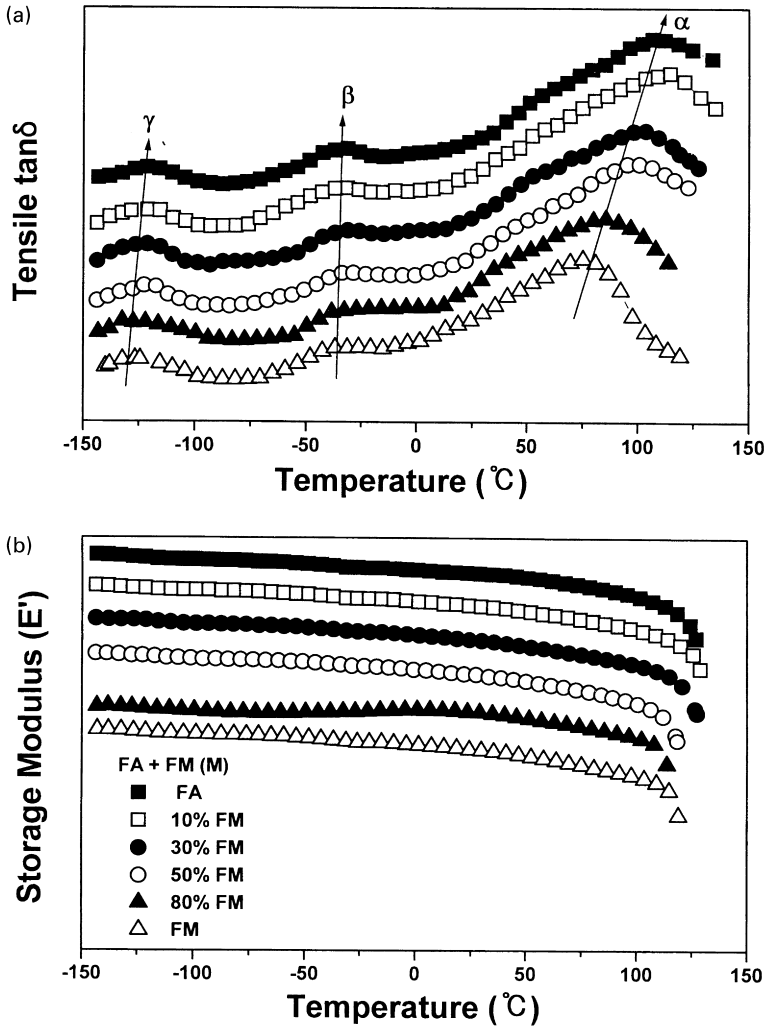

Fig. 6. (a) Tensile tan δ; and (b) storage modulus (E') spectra of melt blended FA + FM. The number indicates the percentage of second component (metallocene catalyzed EOC) in the blends.

(ΔH_c) were obtained from the second scan of the DSC thermogram. The thermal characterization data of the pure polymers are also listed in Table 1.

The viscoelastic properties were measured by using a Polymer Laboratories DMTA Mk III instrument in the range of −145°C to T_m −10°C, in the tensile mode at a constant frequency of 1 Hz and at a heating rate of 2°C/min. The relaxational, α, β, and γ behaviors were analyzed from the tensile storage modulus (E'), the tensile loss modulus (E''), and the tan δ peaks. All the specimens were rectangular-shaped in 10 mm gauge length, 5 mm width and about 0.5 mm thickness.

Torsion rheometric system (Rheometric Scientific) was used to measure the rheological properties. Melt blended samples were heated and pressed in the rheometer at 200°C and held for 5 min to maintain uniform thermal history. A circular parallel plate of diameter 38 mm and constant shear strain were applied at a frequency range of 10^{-1}–10^{2} rad/s and at 200°C. The torsion storage (G') and loss (G'') modulus were measured under sinusoidal stress at various frequency ranges. The complex melt viscosity (η^*), the real part of the complex melt viscosity, i.e. the storage viscosity (η'), and the imaginary part of the complex melt viscosity, i.e. the loss viscosity (η'') were then calculated from the torsion storage modulus.

The mechanical properties of the blends, the tensile strength at yield and break, the elongation at break, and the elastic modulus were measured by an Instron universal testing machine (model 4301) according to ASTM D638-91 after leaving at 25°C and 50% humidity for 48 h. The dimensions of the test specimens were of type IV in ASTM D 638 and the crosshead speed was 200 mm/min.

The morphology of the microtomed cutting surfaces of the blend was observed with a scanning electron microscope (SEM) Jeol JSM-840A at an accelerating voltage of 15 kV. The specimens were microtomed at −100°C and etched by permanganic acid, washed with hydrogen peroxide and distilled water, then coated with gold which is a high conducting material to prevent local charging from the scanning electron beam.

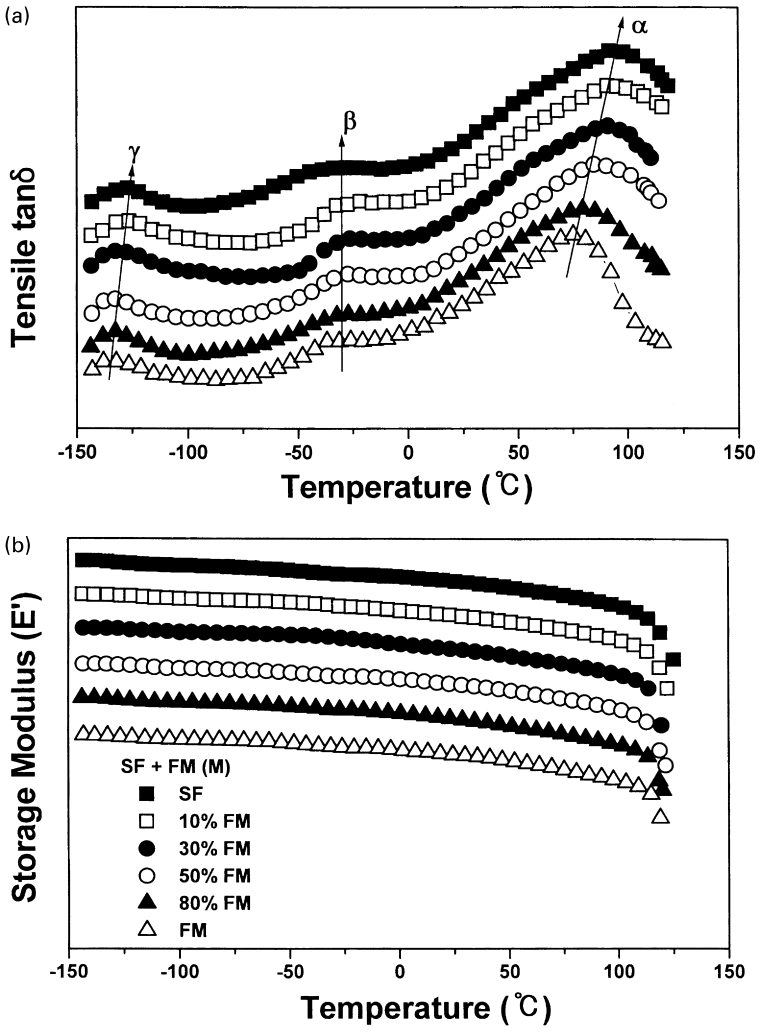

Fig. 7. (a) Tensile tan δ; and (b) storage modulus (E') spectra of melt blended SF + FM. The number indicates the percentage of second component (metallocene catalysed EOC) in the blends.

3. Results and discussion

3.1. Thermal behavior

The melting and crystallization behavior of the melt blended FA + FM are shown in Fig. 2a and b, respectively. The melting points of FA and FM appeared at 123.7 and 111.3°C, respectively. The melting endotherm of FA is broadened and a shoulder between 90 and 115°C is apparent, while that of FM is relatively narrow and sharp. For the blends, two or three melting endotherms are observed, indicating that the blends form separate crystals in the crystallization region. In addition, the melting endotherm of the Ziegler–Natta EOC (i.e. FA) in the blend started separation into two peaks at a composition of 50% FA, while that of metallocene EOC (i.e. FM) broadened and its T_m decreased with the content of metallocene EOC. The crystallization behavior of FA + FM is presented in Fig. 2b. Unlike the melting peak, single or double crystallizing peak was observed.

The melting and crystallization behavior of the solution and melt blended blends can be compared between Fig. 2 (melt blended) and Fig. 3 (solution blended). The melting endotherm and the crystallizing exotherm prepared by solution blending are fairly similar to those obtained by the melt blending except systematic uncertainty. This is in good agreement with the previous studies using the other ethylene copolymers [29].

In Figs. 4 and 5, thermal behavior of the solution and melt blend of SF + FM is depicted, respectively. The melting endotherm for a neat SF (Fig. 4a) shows three distinct melting peaks at 108, 121 and 123°C, indicating that SF is formed with different crystal thickness, while that of FM shows only one peak at 111°C, as seen in Fig. 4a. As a consequence, when SF or FM is molten, three different melting peaks are observed for both the solution and melt blends in Figs. 4a and 5a. On the contrary, unlike the melting behavior, single crystallization peak is observed for all compositions of the blends (Figs. 4b and 5b). In addition, the crystallization peak shifted toward low temperature as

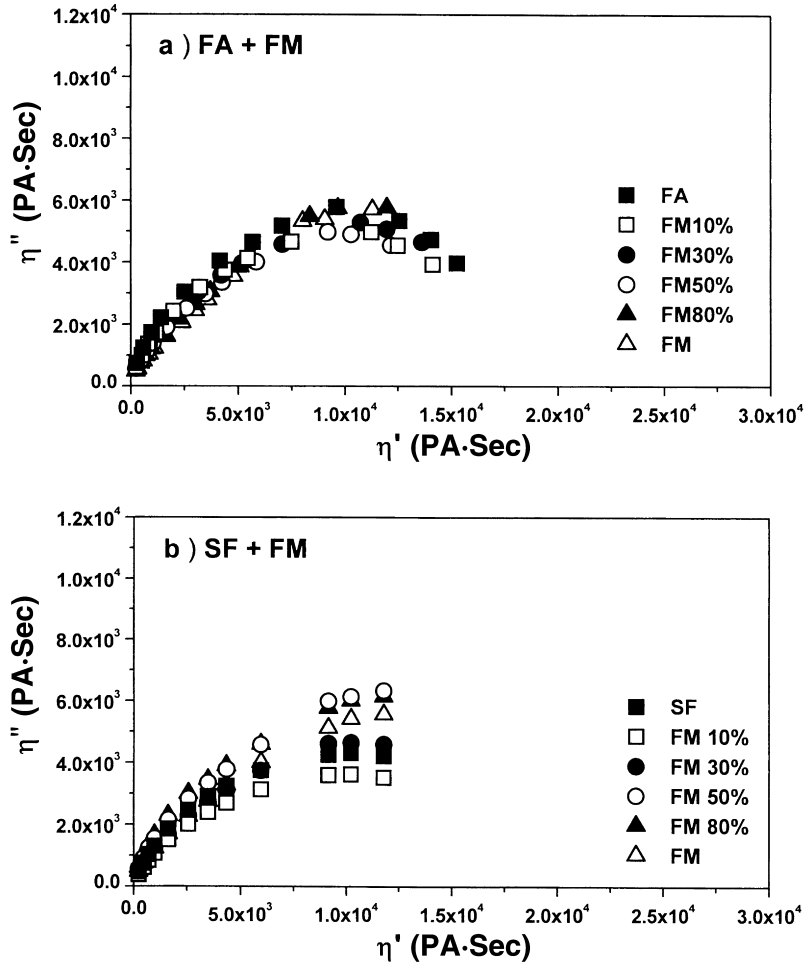

Fig. 8. The Cole–Cole plot, η'' versus η' for: (a) FA + FM; and (b) SF + FM blends.

the content of metallocene EOC (i.e. FM) was increased; this may be due to the metallocene EOC acting as a polymeric diluent.

For our investigated EOC blends, the DSC measurements thus indicate that two EOCs exclude one another during crystallization process regardless of the blending manners. This is rather surprising, particularly for the FA + FM blend, since FA and FM have similar MI, density, and comonomer content. As seen in Fig. 1, although the side chain content between FA and FM is similar, and that between SF and FM is different, the side chain distribution between the former and the latter two components is different. In addition, the relative molecular weight of the metallocene EOC is larger than the Ziegler–Natta EOCs. Hence the key factor for representing phase separation would be the difference in the side chain distribution and the length of the side chain caused by the different catalysts for the synthesis of each constituent. In addition, the phase separation for the blend of SF + FM may also be rationalized by the same points as discussed for the FA + FM blend. In our previous study, the thermal study of LLDPE blend with conventional LDPE showed the formation of separate crystals in the crystalline region, but miscibility was observed in the amorphous region [26]. Ziegler–Natta EOCs used in this study belong to the conventional LLDPE, while the metallocene EOC and the conventional LDPE have the similar trend in the length of the side chain. Recently, the interaction parameter between the polyolefin components has been directly calculated by various techniques [30–33]. Thus the future work would be the calculation of the interaction parameters using the above techniques.

3.2. Viscoelastic property

The crystallinity, lamellar thickness, and interfacial structure of polyethylene influence the viscoelastic behavior of it. Since the mechanical relaxation spectra of melt and solution blended samples appeared to be very similar, the DMTA thermograms of the FA + FM and SF + FM blends prepared by melt blending only are shown in Figs. 6 and 7, respectively, in the temperature range of −150 to 150°C. For the pure resins, FA, SF and FM, the common feature is the observation of the relaxational α, β, and γ transitions, where the α transition occurs at about 105, 100 and 75°C,

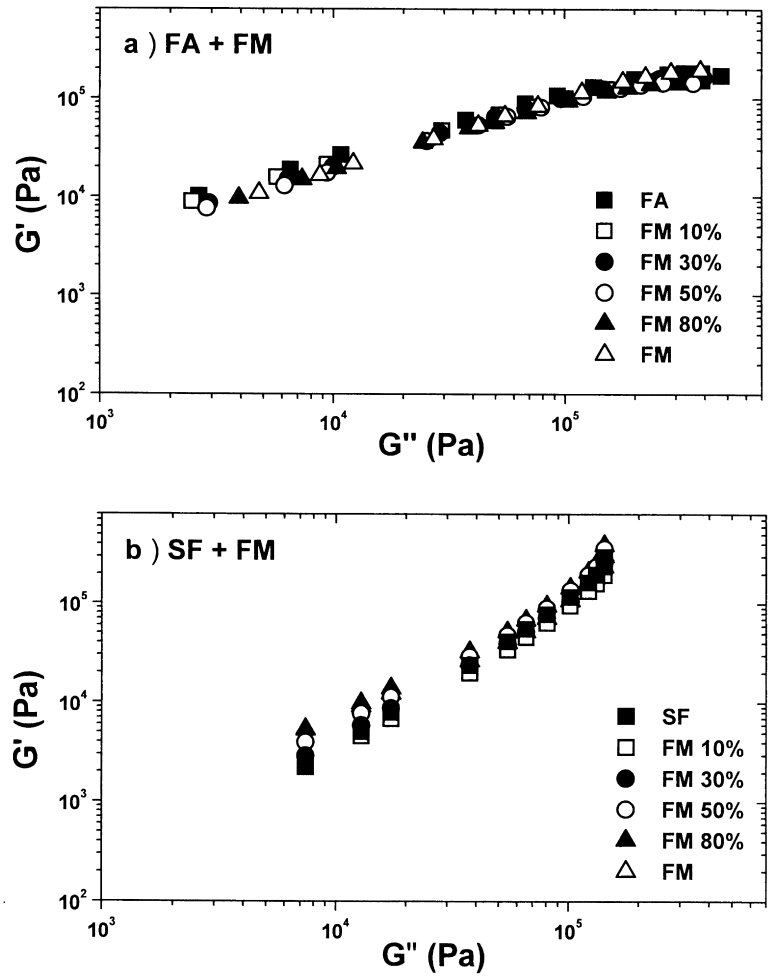

Fig. 9. The log G' versus log G'' plot for: (a) FA + FM; and (b) SF + FM blends.

β at about −36, −37, and −36°C, and γ at about −126, −125, and −130°C, respectively. The low temperature γ relaxation, which is defined as the glass transition temperature of polyethylene [26], exhibits a single transition without any variation within a narrow range of temperature between −125 and −130°C. Like the γ transition, the β relaxation exhibits a single transition in the same position. This may have arisen from the same comonomer that is 1-octene. In our previous study [26], we claimed that the β relaxation is a reflection of not only the degree of crystallinity but also the length of the side-chain branching and the comonomer content. The latter was varied due to the maximum position of the transition or the area of the transition region. Regarding α ralaxation, the metallocene EOC (FM) shows lower melting than those of the Ziegler–Natta catalyzed EOCs, FA and SF. For the blends of FA + FM and SF + FM, a broad single α peak appeared and the maximum position linearly decreased with an increase in the FM component.

3.3. Melt rheology

Since the specimens prepared by melt and solution blending showed similar behavior, rheological properties of two blends, FA + FM and SF + FM are carried out by using the melt blend only. As expected, the complex melt viscosity (η^*) decreased with angular frequencies indicating a non-Newtonian behavior. Similar behavior is observed for the storage viscosity (η') and loss viscosity (η''). To analyze the rheological data, we used three different techniques: the first is the Cole–Cole plot in which η'' versus η' is plotted [34]. The FA + FM blends of all compositions showed almost the same diameter of the semicircle as seen in Fig. 8(a). Further, in the case of the SF + FM blends, the plot has a trend to reach a semicircle with different diameters for various blend compositions as shown in Fig. 8(b).

The second technique is the plot of log G' (storage modulus) versus log G'' (loss modulus), which is developed by Han et al. [35] and is useful to differentiate polymer–polymer miscibility. In this method, if the blend composition gives the same slope with that of the pure component, then the blend is interpreted to be miscible. On the contrary, for immiscible or phase separated blend, the blend composition gives different slope from that of the pure components. Such plots for the FA + FM and SF + FM blends

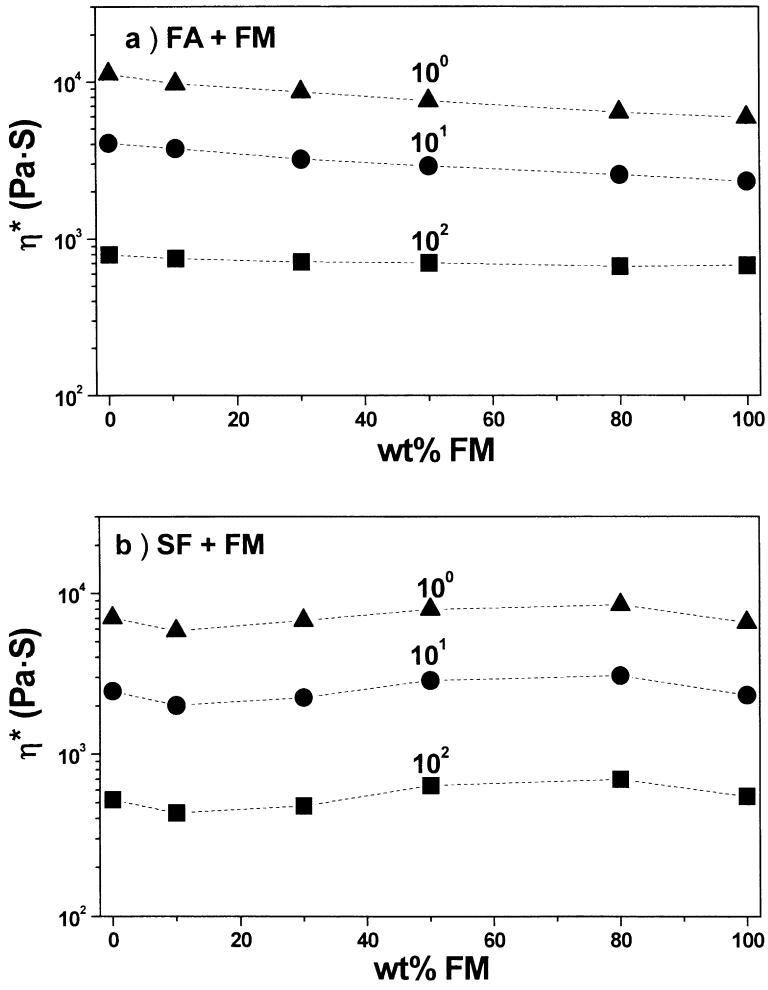

Fig. 10. The log complex melt viscosity (η^*) as a function of the blend composition for: (a) FA + FM; and (b) SF + FM. The symbols are the same for two blends: ▲, 10^0 rad/s; ●, 10^1 rad/s; and ■, 10^2 rad/s.

are presented in Fig. 9. In Fig. 9(a), the slopes of the FA + FM blend are almost the same as those of the pure components indicating a miscibility, whereas in SF + FM, slightly scattered and upward tailing are seen implying a phase separation in the melt state.

The third technique is a plot of the log complex melt viscosity (η^*) versus the blend composition [36]. In Fig. 10(a) for FA + FM, a linear log–log plot is observed, while for SF + FM, the plots are curved with negative as well as positive deviation from the average values. There

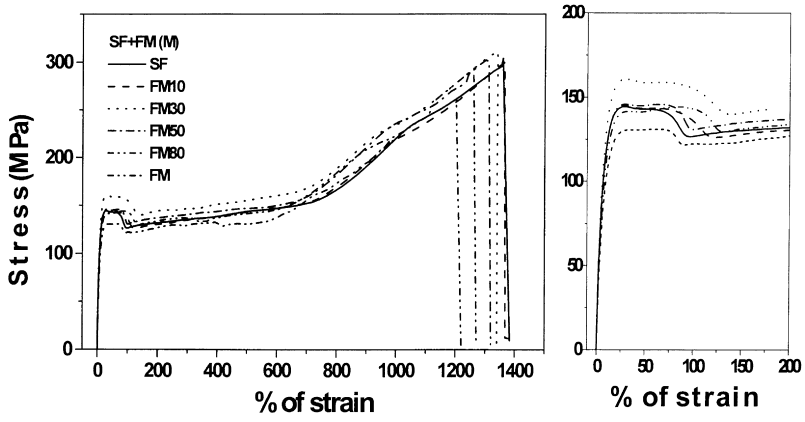

Fig. 11. Stress–strain curves of the SF + FM blend with the yield region of the blend enlarged.

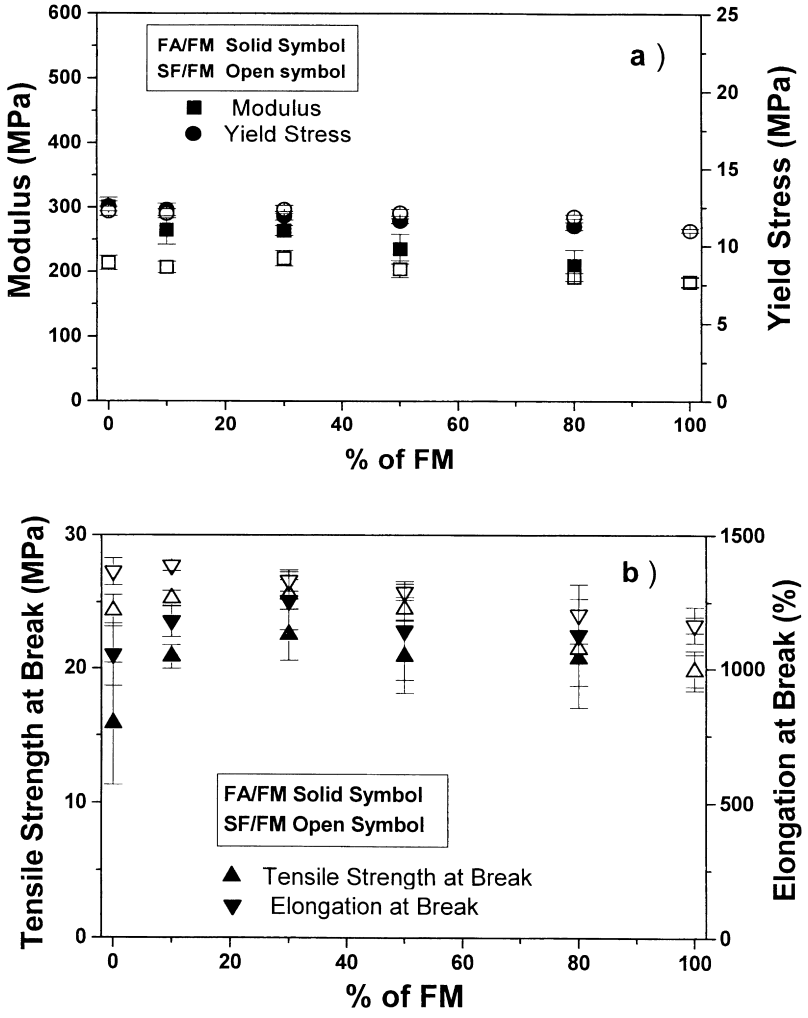

Fig. 12. Modulus, yield stress, ultimate stress, and elongation at break as a function of FM content in FA + FM and SF + FM.

are many reports in literatures; positive deviation blending (PDB) is observed in the immiscible HDPE/poly (ethylene-*co*-vinyl acetate) (EVA) blends. Yang et al. [37] demonstrated that melt viscosity at zero shear rate (η_0) versus the blend composition at constant temperature showed negative deviation blending (NDB) for miscible PMMA/poly (vinylidene fluoride), but PDB for miscible PMMA/poly (styrene-*co*-acrylonitrile). According to their remarks, T_g for amorphous polymer and T_m for semi-crystalline polymer should be selected as reference temperature. Regarding on our systems, two constituents comprised of hydrocarbons do not have any specific interactions. Hence from the above three different techniques, the FA + FM blend seems to be miscible, while the SF + FM one seems to be immiscible in the melt state, suggesting that the comonomer content in the blends influences the rheological properties in the melt state.

3.4. Mechanical property

The stress–strain behavior of the blends of FA + FM and SF + FM is measured and representative plots are shown in Fig. 11. On the right-hand side, the stress in the small range of strain up to 200% is enlarged. As seen in this figure, yielding and cold drawing were observed with a necking behavior. In Fig. 12, the tensile properties such as the elastic modulus, the yield stress, the ultimate stress and the maximum elongation at break are depicted. For both the blends, the modulus and the yield stress followed the rule of mixtures (in Fig. 12a), whereas for the ultimate stress and the elongation at break, slightly synergistic behavior was observed at 10–60% FM for FA + FM, but linearity was observed for SF + FM in Fig. 12b. As a consequence, the difference in the distribution of the side chain branching and the length of the side chain do not influence notably of the mechanical properties of the blends.

3.5. Morphological behavior

The morphology of the melt and solution blended samples is presented in two different cooling rates, which are fast and slow cooling processes. When cooling rate is

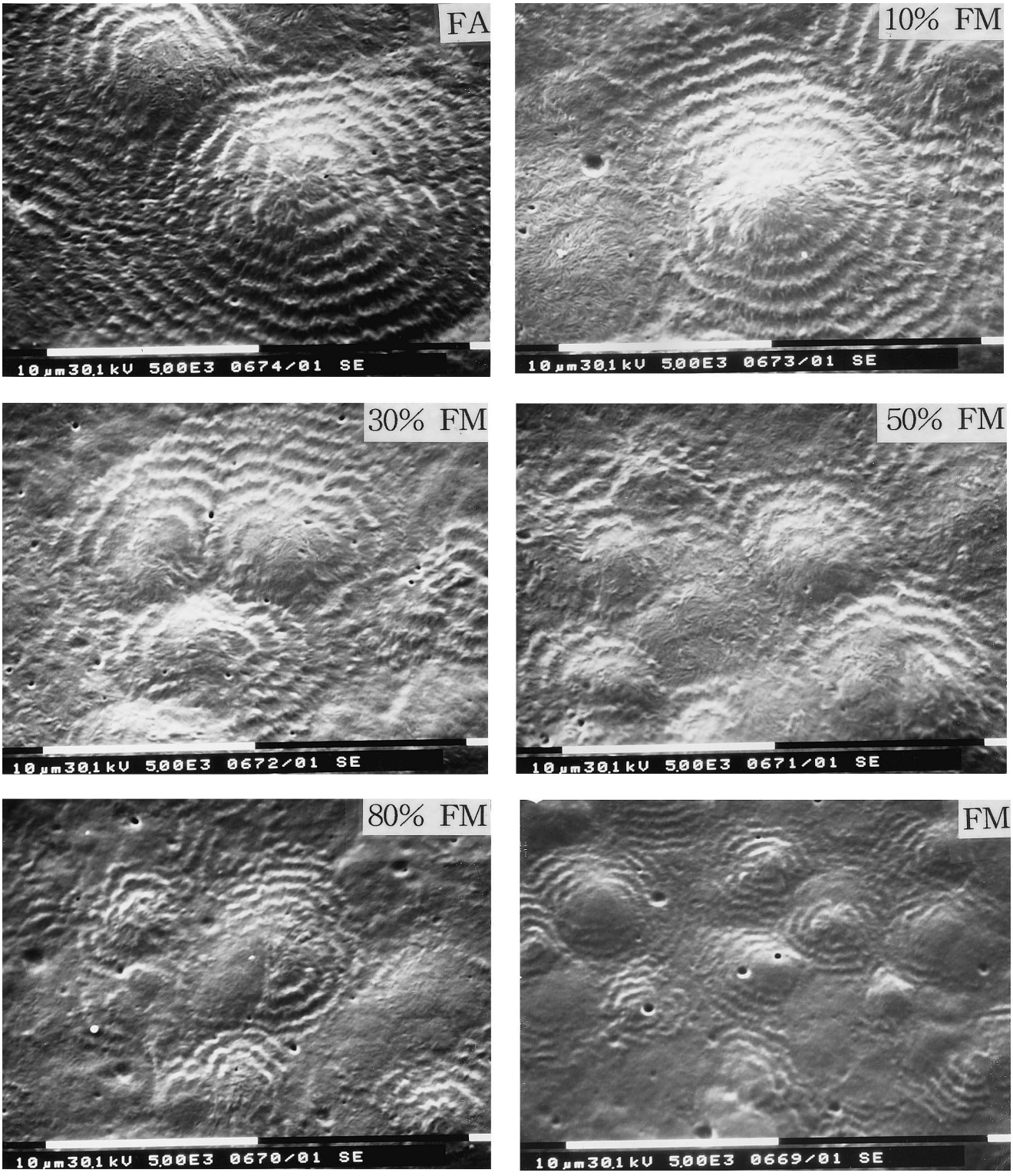

Fig. 13. Scanning electron microscopic photographs of microtomed cutting surfaces of slow cooled materials by melt blending: (a) FA + FM (M); (b) SF + FM (M).

fast, the spherulites are much reduced in size compared to those from slow cooling, hence morphological behavior discussed in this article is on the samples prepared by the slow cooling solely. In Fig. 13(a) and (b), melt blended FA + FA (M) and SF + FA (M) are compared, respectively. The size of the spherulitic diameter of FA is more than 40 μm exhibiting characteristic banding pattern with a spacing of 1–1.5 μm. On the contrary, that of SF is between

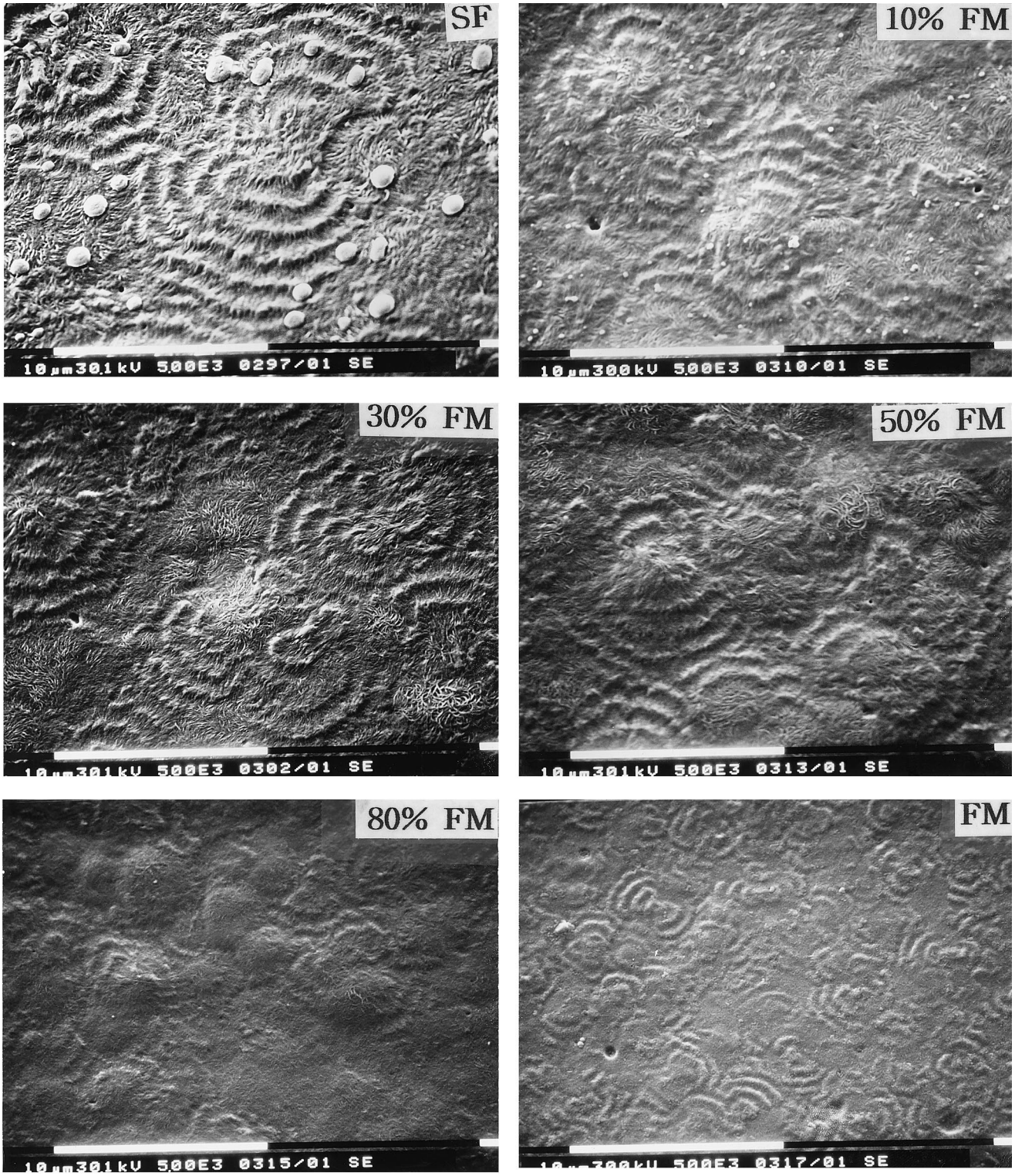

Fig. 13. (*continued*)

10 and 15 μm, while that of FM is less than 5 μm. For the blends, the diameter of the banded spherulites linearly decreased with the FM content.

For solution blending specimens in Fig. 14(a) and (b), the size of the banded spherulites of FA and SF decreased compared to that by melt blending, whereas that of FM was enlarged up to 15–20 μm. However, similar diameter of the banded spherulites formed in all the blend compositions of the two blends, FA + FM (S) and SF + FM (S).

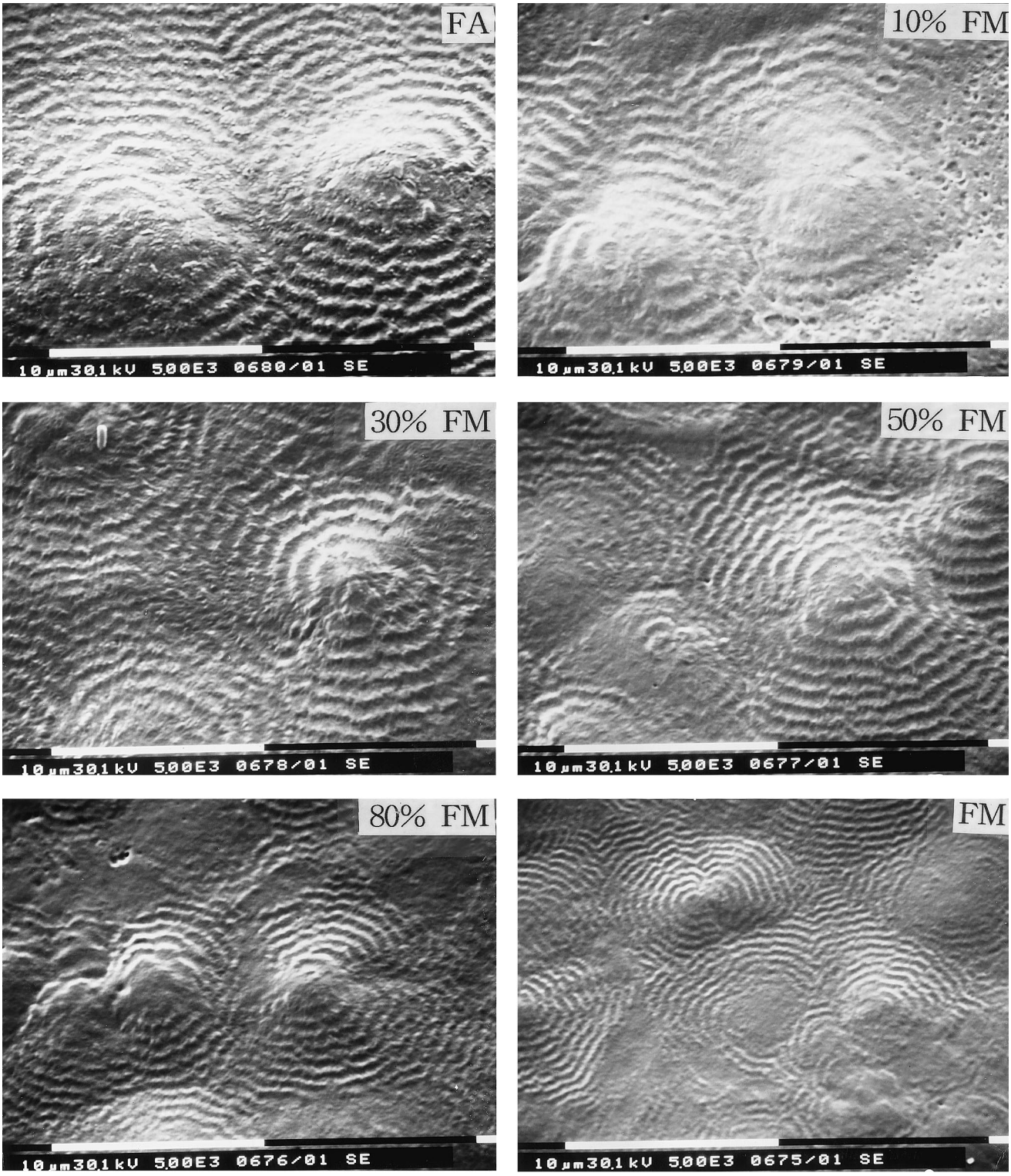

Fig. 14. Scanning electron microscopic photographs of microtomed cutting surfaces of slow cooled samples by solution blending: (a) FA + FM (S); (b) SF + FM (S).

Between Figs. 13 and 14, we can observe an interesting feature. For both the blends, FA + FM and SF + FM, the size of the banded spherulites of FA or SF prepared by melt blending decreased compared with that prepared by solution blending, however, the inverse behavior was observed in FM. This indicates that the nucleation growth of FM in a solution blending is faster than in melt blending process.

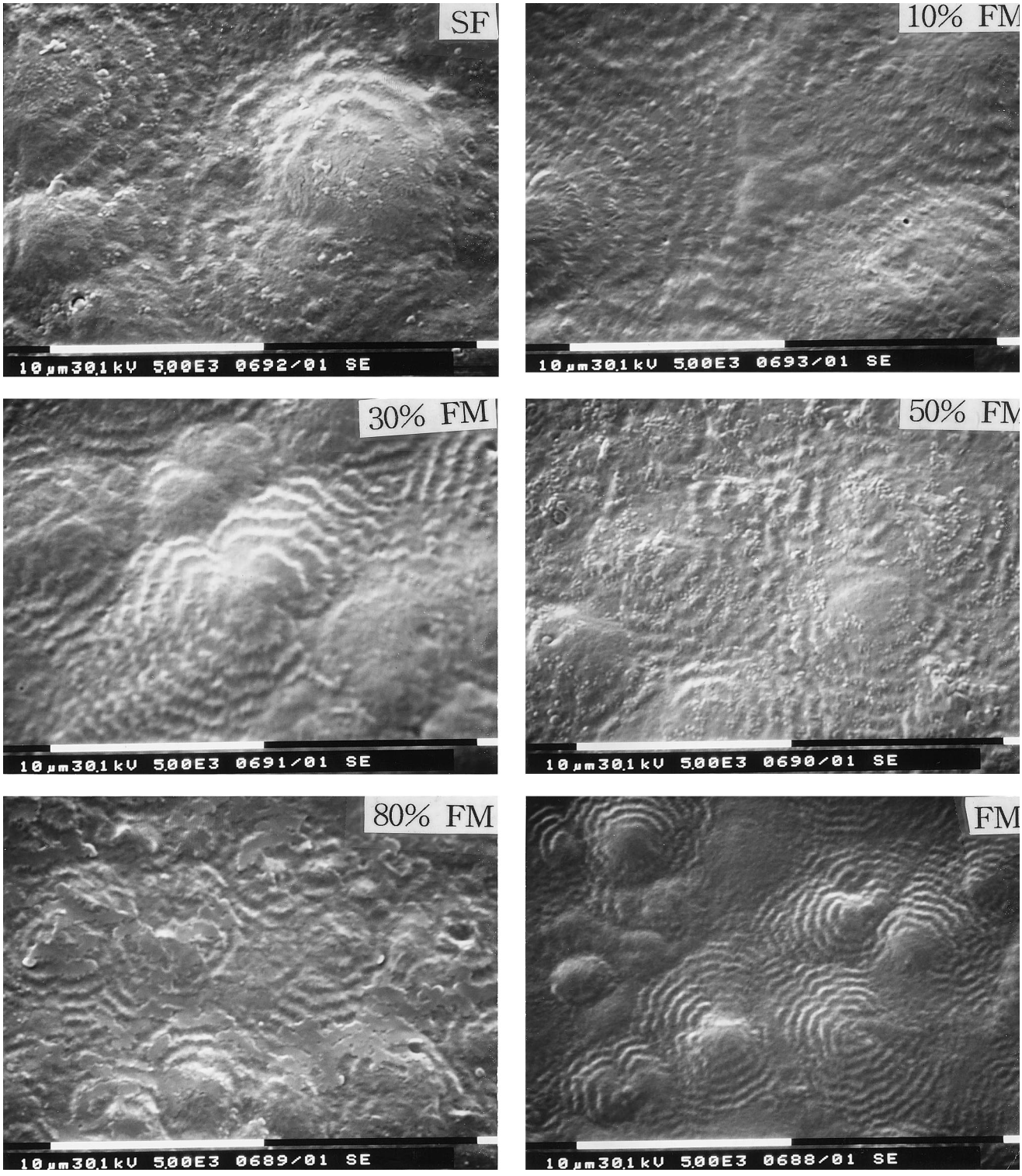

Fig. 14. (*continued*)

4. Conclusions

Miscibility and phase morphology of two pairs of the Ziegler–Natta and metallocene catalyzed EOC blends have been studied in terms of the thermal, viscoelastic, rheological, mechanical and morphological properties. One pair consists of components with similar MI, density and comonomer content, and the other consists of similar MI and density, but different comonomer content. The main difference between the neat Ziegler–Natta and the metallocene EOCs is the distribution and the length of the side chain branchings. Thermal studies of melt and solution

blended specimens show multiple melting or crystallizing peaks indicating that the constituents exclude one another in the crystallization state and that no dependency of the blending method is observed. Viscoelastic properties indicate that the blends are miscible in the amorphous region on account of the observation of a single peak of γ relaxation. The melt rheology suggests that FA + FM be miscible, while SF + FM be immiscible in the molten state. The mechanical properties analyzed in terms of the elastic modulus, the yield stress, the ultimate stress and the elongation at break showed similar properties without distinctive variations. Phase morphology of the two blends prepared by the melt blending with slow cooling process indicates that bigger spherulitic diameter and ring space are observed in the Ziegler–Natta EOCs. In particular, grass like spherulitic sheaf structure is dominated in the blend by an incorporation of the metallocene EOCs. On the contrary, for the samples prepared by solution blending, the spherulites of the Ziegler–Natta EOCs decreased, while those of the metallocene EOC increased. Thus for the hybrid blends consisting of similar MI and density, it is suggested that the difference in miscibility between the molten and solid states be influenced by not only the distribution of the side chain branching but also the length of the side chains.

Acknowledgements

Financial support from SK Corporation is gratefully appreciated. S. Choe particularly sends appreciation to Mr Uhm of Sam Gung General Chemicals for measuring the side chain distribution of the polyolefins.

References

[1] Donatelli AA. J Appl Polym Sci 1979;23:3071.
[2] Hu SR, Kyu T, Stein RS. J Polym Sci, Polym Phys Ed 1987;25:71.
[3] Kyu T, Hu SR, Stein RS. J Polym Sci, Polym Phys Ed 1987;25:89.
[4] Ree M, Kyu T, Stein RS. J Polym Sci, Polym Phys Ed 1987;25:105.
[5] Mirabella FM, Westphal SP, Fernando PL, Ford EA, Williams JG. J Polym Sci, Polym Phys Ed 1988;26:1995.
[6] Hay JN, Zhou X-Q. Polymer 1993;34:2282.
[7] Gupta AK, Rana SK, Deopura BL. J Appl Polym Sci 1992;44:719.
[8] Gupta AK, Rana SK, Deopura BL. J Appl Polym Sci 1993;49:477.
[9] Gupta AK, Rana SK, Deopura BL. J Appl Polym Sci 1994;51:231.
[10] Tashiro K, Izuchi M, Kobayashi M, Stein RS. Macromolecules 1994;27:1221.
[11] Tashiro K, Izuchi M, Kobayashi M, Stein RS. Macromolecules 1994;27:1228.
[12] Tashiro K, Izuchi M, Kobayashi M, Stein RS. Macromolecules 1994;27:1234.
[13] Dharmarajan NR, Yu TC. Plastics Engng 1996;52:33.
[14] Woo L, Ling MTK, Westphal SP. Thermochim Acta 1996;272:171.
[15] Westphal SP, Ling MTK, Woo L. Thermochim Acta 1996;272:181.
[16] Bensason S, Minick J, Moet A, Chum S, Hiltner A, Baer E. J Polym Sci, Polym Phys Ed 1996;34:1301.
[17] Bensason S, Nazarenko S, Chum S, Hiltner A, Baer E. Polymer 1997;38:3513.
[18] Vega JF, Munoz-Escalona A, Santamaria A, Munoz ME, Lafuente P. Macromolecules 1996;29:960.
[19] Munoz-Escalona A, Lafuente P, Vega JF, Munoz ME, Santamaria A. Polymer 1997;38:589.
[20] Lee SY, Jho JY. J Ind Engng Chem 1998;4:170.
[21] Voigt-Martin IG, Alamo R, Mendelkern L. J Polym Sci, Polym Phys Ed 1986;24:1283.
[22] Defoor F, Groeninckx G, Reynaers H, Schouterden P, Van der Heijden B. Macromolecules 1993;26:2575.
[23] Cho K, Lee H, Lee BH, Choe S. Polym Engng Sci 1998;38:1969.
[24] Cho K, Ahn TK, Lee BH, Choe S. J Appl Polym Sci 1997;63:1265.
[25] Cho K, Ahn TK, Park I, Lee BH, Choe S. J Ind Engng Chem 1997; 3:147.
[26] Lee H, Cho K, Ahn TK, Choe S, Kim IJ, Park I, Lee BH. J Polym Sci, Polym Phys Ed 1997;35:1633.
[27] Rana D, Lee CH, Cho K, Lee BH, Choe S. J Appl Polym Sci 1998;69:2441.
[28] Rana D, Lee CH, Choe S, Cho K, Lee BH. Korean Polym J 1998; 6:158.
[29] Bensason S, Nazarenko S, Chum S, Hiltner A, Baer E. Polymer 1997; 38:3913.
[30] Alamo RG, Londono JD, Mandelkern L, Stehling FC, Wignall GD. Macromolecules 1994;27:411.
[31] Graessley WW, Krishnamoorti R, Balsara NY, Butera RJ, Fetters LJ, Lohse DJ, Schulz DN, Sissano JA. Macromolecules 1994;27:3896.
[32] Wignall GD, Londono JD, Lin JS, Alamo RG, Galante MJ, Mandelkern L. Macromolecules 1995;28:3156.
[33] Alamo RG, Graessley WW, Krishnamoorti R, Lohse DJ, Londono JD, Mandelkern L, Stehling FC, Wignall GD. Macromolecules 1997; 30:561.
[34] Cole KS, Cole RH. J Chem Phys 1941;6:341.
[35] Han CD, Kim J. J Polym Sci, Polym Phys Ed 1997;25:1741.
[36] Utracki LA, Kamal MR. Polym Engng Sci 1982;22:96.
[37] Yang HH, Han CD, Kim JK. Polymer 1994;35:1503.